ICONHIC 2016
1st International Conference on Natural Hazards & Infrastructure
28-30 June, 2016, Chania, Greece

MSE: a Resilient Retaining System

I. Georgiou[1], F. Gelagoti, R. Kourkoulis, G. Gazetas
National Technical University of Athens

ABSTRACT

During the last decades the need for less conservative geotechnical design and for a Performance Based approach encourages a paradigm shift in geotechnical applications by implementing the concept of sustainable engineered systems. Resiliency, efficiency and cost-effectiveness are key factors that support this approach. Considering earth retaining walls, the concept of mechanically stabilized earth (MSE) could combine the above attributes, while being environmentally friendly and adaptive to a variety of construction conditions. Natural hazards, such as earthquakes, may prove crucial for the design of MSE systems, since their robustness and reliability depend on their performance under such unprecedented events.This paper aims to comparatively study the seismic response of a MSE steel-reinforced vs. concrete-reinforced retaining wall. The MSE system is composed of welded steel meshes which internally enhance the capacity of the soil backfill. Fully non-linear 2-dimensional numerical analyses are carried out with emphasis on the interface conditions. Results demonstrate the superior performance of the reinforced earth system as compared to the concrete one, both in terms of accumulated displacements and structural integrity, especially when subjected to strong seismic excitations.

Keywords: resilience, mechanically stabilized earth, retaining wall, seismic, performance based design, sustainability

INTRODUCTION

The need to shift geotechnical design from a "factor of safety" to a "performance based" design (PBD) approach has increased rapidly in the past years following examples from structural engineering. In early practice, the only criterion for achieving good performance was to avoid failure; designers had only to ensure that the available capacity of the geotechnical system is sufficiently higher than the expected demand (i.e. Load and Resistance Factor Methodologies). Yet, even when the key design requirements against collapse are satisfied, the system may still be placed into a condition in which the deformation constraints are not met (Bolton, 2012). To address these issues, geotechnical design has been moving to a predominantly performance-based approach that correlates deformation considerations to the severity of the experienced loading. As such, in earthquake-related problems, the definition of good performance of a geotechnical system is no more unique; for a low intensity earthquake the system should remain serviceable (i.e. the developed deformations should remain low), whilst for the design earthquake the maintenance of life-safety is the sole performance criterion.

Yet, this is still not enough. During the last 20 years, the examples of recorded earthquakes that overly exceed the design standards keep increasing. A merely indicative list of very recent events should include the Wenchuan (2008) earthquake, the fatal M8.8 Chile (2010) earthquake and the triple earthquake events that consecutively shook Christchurch New Zealand with recorded accelerations in the order of 1g. Attempting to

[1] Corresponding Author: I.A. Georgiou, *National Technical University of Athens, irelimni@outlook.com*

design for such unprecedented seismic actions would certainly impose enormous demands to the structure and would provoke a ludicrous squander of resources. Recognition of our inherent inability to control nature (especially when resources are limited) has led the engineering community to pursue resilience as the most viable strategy to minimize the consequences of the inevitable disaster (Bruneau and Reinhorn, 2007). Resilience is often defined in terms of the ability of a system to absorb shocks, to avoid crossing a threshold into an alternate and possibly irreversible new state, and to regenerate after disturbance (Resilience Alliance 2009). In the words of Holling (1996), a resilient system may be disturbed and still persist without changing function.

This paper aims at highlighting the application of the idea of resilience in the design of Earth Retaining Systems. A key challenge is that by definition our problem lacks measurable performance metrics. To overcome this obstacle, we have envisioned a direct comparison of two conventionally equivalent retaining structures: a typical pile-wall system and a MSE wall.

Since the first Mechanically Stabilized Earth (MSE) wall construction in California in the early 70's, MSE systems have become increasingly popular due to their low cost and ease of construction especially when it comes to 'deep cuts'. Among their other important attributes, MSE systems have been found to have equal or better performance than more rigid wall systems under seismic loading events. In strength-based terminology both retaining systems are treated as totally equivalent; both are designed to attain identical Seismic Factors of Safety. These two 'equivalent' structures are here subjected to a variety of loading scenarios and the Resilience is judged on the basis of their ability:

(a) to remain functional after medium-intensity earthquakes
(b) to preserve their structural integrity under extremely strong earthquake events (far in excess of the design-earthquake)
(c) to demonstrate redundancies

PROBLEM DEFINITION AND NUMERICAL MODELING

The problem under investigation refers to a retaining wall supporting a 10m-height backfill. Two alternatives were examined and compared in the sequence, consisting of:

a. a conventional bored pile retaining wall
b. a steel-reinforced Mechanically Stabilized Earth (MSE) wall

The geometry and main characteristics of the two alternatives are schematically illustrated in Fig.1. Following the currently applicable code approach, the compared systems were designed so as to ensure the same static and seismic (pseudo-static) safety factors. Hence, an equivalence in static and seismic safety factors (FS_{static}= 1.8 and $FS_{seismic}$ =1.2 assuming a design ground acceleration of 0.16g) is achieved by the following alternatives:

a. Tangent pile wall with pile diameter of 1.2m (ultimate moment capacity M_{ult} = 1.7MNm) and 20m height, 10m of which is the free wall height and 10m the embedded part.
b. Rows of 7m – long reinforcement grids at 0.6m vertical spacing. The grid configuration consists of 10mm bars at 20cm spacing both in the longitudinal and the transverse direction.

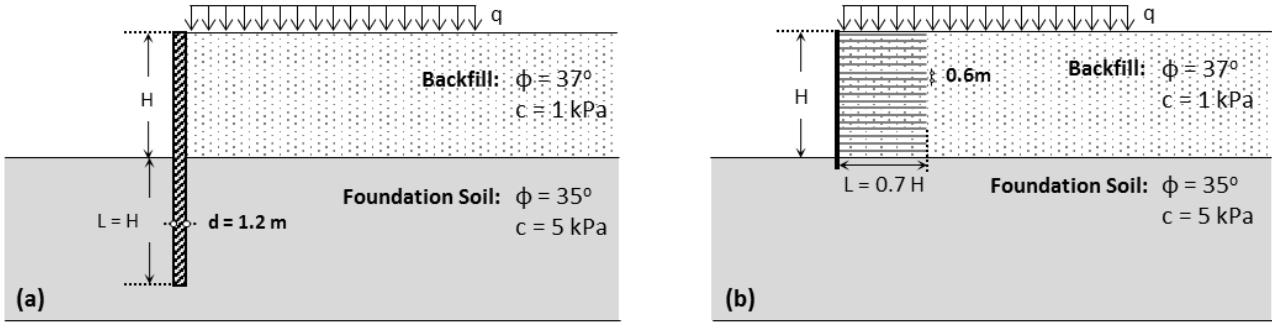

Figure 1. Geometry of the examined retaining systems: (a) conventional bored pile wall and (b) Mechanically Stabilized Earth

Utilizing the finite element codes ABAQUS and PLAXIS, the analysis is conducted assuming plane strain conditions and taking account of material and geometric nonlinearities. As illustrated in Fig. 2, the geometry is "mirrored" in order to ameliorate the lateral boundary effects and examine the effect of the inherent asymmetry of the accelerogram in a single dynamic analysis. The soil is modeled with nonlinear continuum elements, while 2D beam elements, circumscribed by plane-strain continuum elements of nearly zero stiffness, are used to model the piles. Thus, pile stiffness is introduced in the simulation through the central beam element, the nodes of which are rigidly connected with the circumferential solid element nodes at the same height. The Moment-curvature relationship obtained from section analysis, serves as input parameter for the proper simulation of the non-linear response of the concrete pile wall. Sliding and detachment of the pile from the surrounding soil can be captured through special interface elements placed at the pile periphery.

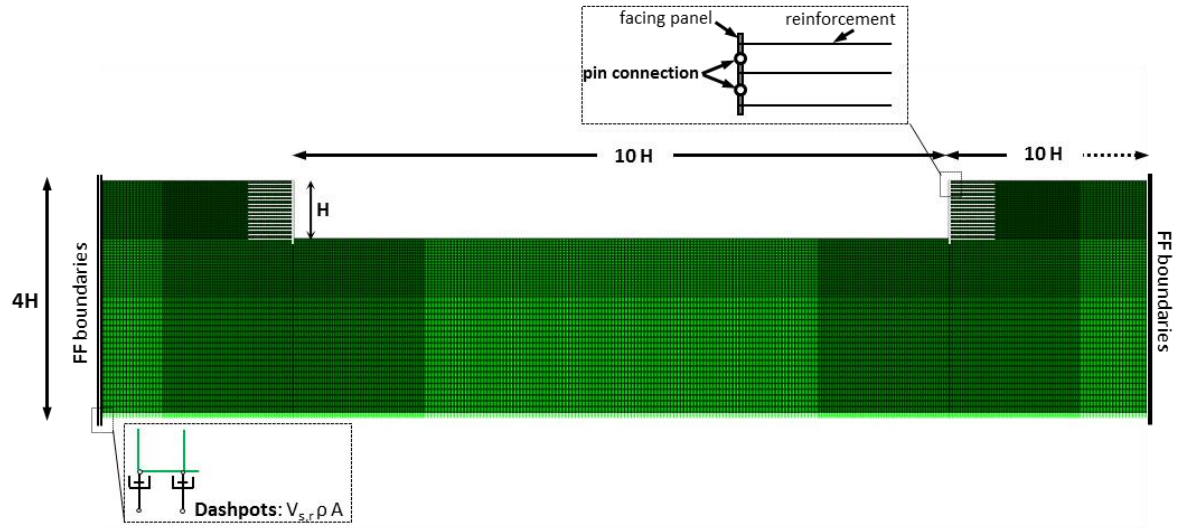

Figure 2. Finite element model of the MSE wall

Concerning the MSE model, continuum and truss elements are used for the concrete facing panels and the grid reinforcements respectively. Each facing panel (0.2m in thickness and 0.6m in height) is connected with its neighboring panels with a pinned connection. The latter allows relative rotation between panels, but restricts the horizontal and vertical degrees of freedom. Thus, the actual connection between consecutive panels is simulated as realistically as possible. The truss elements simulating the steel reinforcement are in turn connected to individual facing panels.

As has been proven by means of several pull-out tests of grid steel reinforcements, the apparent friction coefficient f* at the sand/mesh interface decreases with the increase of embankment height. This phenomenon is characteristic of the behavior of dilatant materials under low confining stresses and is attributable to the presence of the grid which restrains the sand's tendency to dilate. According to Lajevardi et. al. (2013), f* decreases from the value of 1 at the surface to approximately 0.6 at the depth of 6m, while it remains constant for larger depths. This trend is in agreement with French standard provisions (NF P 96-270, 2009) which prescribe f* values of 0.9 and 0.4 respectively. This study assumes the truss elements (representing the reinforcement grid) to be in perfect contact with the surrounding soil elements. This means that the coefficient of friction at the soil-reinforcement interface is equal to $f^* = \tan\varphi = 0.75$, (where φ is the internal friction angle of the backfill) which apparently –based on the aforementioned values- is quite conservative for the upper rows of reinforcement. Understandably, lower f* values at the top layers of the MSE wall (where the length of the resisting (anchoring) zone is smaller) are expected to over-predict seismic displacements. However, this value has been deliberately maintained low in an attempt to showcase the inherent resilience of MSE systems as described in the ensuing.

The behavior of the soil is modeled through a modified kinematic hardening constitutive model, encoded in the Abaqus environment through a user subroutine. Developed by Anastasopoulos et al. (2011), it combines an extended pressure-dependent Von Mises failure criterion, with nonlinear kinematic hardening and associated plastic flow rule. The evolution law consists of two components: a nonlinear kinematic hardening component describing the translation of the yield stress in the stress space, and an isotropic hardening component which defines the size of the yield surface σ_0 as a function of plastic deformation. Details can be

found in the afore-cited reference. For the purposes of the present study, model parameters were systematically calibrated for various levels of the overburden stress according to the experimental G-γ and ξ-γ curves of Ishibashi & Zhang (1993). The shear modulus G_0 at small strains was estimated according to the expression of Seed et al. (1986):

$$G_0 = 1600\, K_2\, (\sigma_m)^{0.5} \quad (1)$$

where σ_m is the confining pressure while parameter K_2 is a characteristic of the soil and was taken equal to 10, for the relatively dense sand adopted herein.

Interfaces between facing panels and soil, as well as between piles and soil are modeled with special contact elements that allow both separation and slippage, the latter controlled by coefficient of friction μ=0.7. Proper kinematic constraints have been assumed at the lateral boundaries of the FE model to simulate free-field response, while dashpot elements have been used at the base of the model to correctly reproduce radiation damping.

RESULTS

Performance under static loading

Before proceeding to the dynamic analyses, the retaining systems were examined under static loading. Note that construction sequence was not simulated and the models are assumed to be wished-in-place. This assumption, in accord with previous studies, has proven more conservative for the MSE system, since it overestimates both the plastic strains and the displacements at the facing.

Horizontal deformations under static loading, which consists of the application of gravity in conjunction with a uniformly distributed load of 10kN/m along a distance of 50m behind the wall, are represented in Fig 3. Although equivalent in terms of safety factors, the flexibility of the pile system is prominent, exhibiting an approximately 3-fold larger displacement (3cm) compared to the MSE alternative (1cm). Interestingly, more pronounced is the difference in the mode of deformation: deformations of the pile system decrease linearly with depth until the level of excavation and remain almost constant along the embedment part; on the contrary, the maximum lateral deformation of the MSE takes place in the middle of its height, resulting in a convex deformed shape of the facing. The latter is in agreement with findings of experimental studies (Suberhamani et al. 2008), thus providing confidence in the adopted numerical methodology.

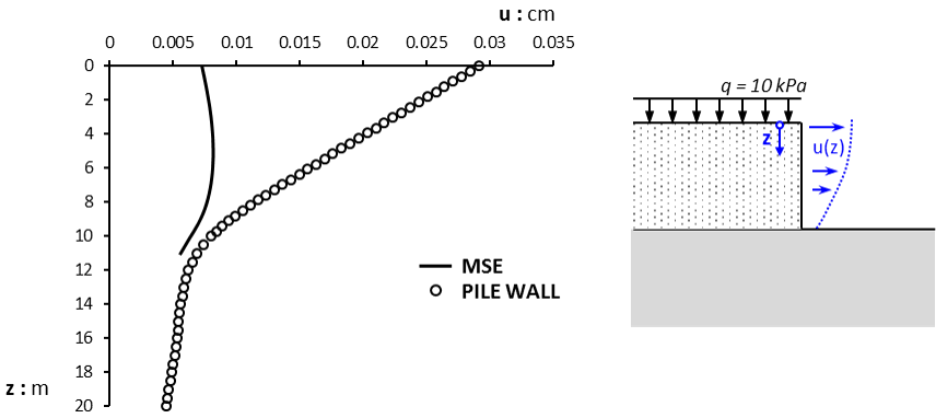

Figure 3. Distribution of the horizontal displacements under static loading

Seismic excitation: wall deformation and damage

As already stated, resilience of retaining systems depends on their performance under extreme events, such as unprecedented earthquakes probably even beyond their design. To this end, this section compares the response of the two well-designed systems presented previously under moderate and high-intensity earthquake scenarios.

In order to cover a range of realistic seismic motion characteristics, seismic performance is investigated using four recorded accelerograms. The selected earthquake scenarios can be classified according to their frequency content into two categories: the high-frequency motions where the great portion of the earthquake energy corresponds to periods (T) lower than 0.3s and the low-frequency motions, where spectral accelerations are maximized for periods greater than 0.75 s. Their acceleration time histories along with their elastic response spectra are plotted in Fig.4. The LPCC record of the 2011 M_s 6.3 Christchurch earthquake and the Gilroy record of the 1989 M_s 7.1 Loma Prieta earthquake belong to the first category, with maximum accelerations of 0.9g and 0.4g, respectively. The second one contains the 2003 M_s 6.4 Lefkada (Greece) earthquake record, characterized by a sequence of roughly eight strong motion cycles with PGA =0.4g, and the well-known Rinaldi (228) record of the 1994 M_s 6.8 Northridge earthquake which is characterized by forward-rupture directivity effects, with PGA=0.8g.

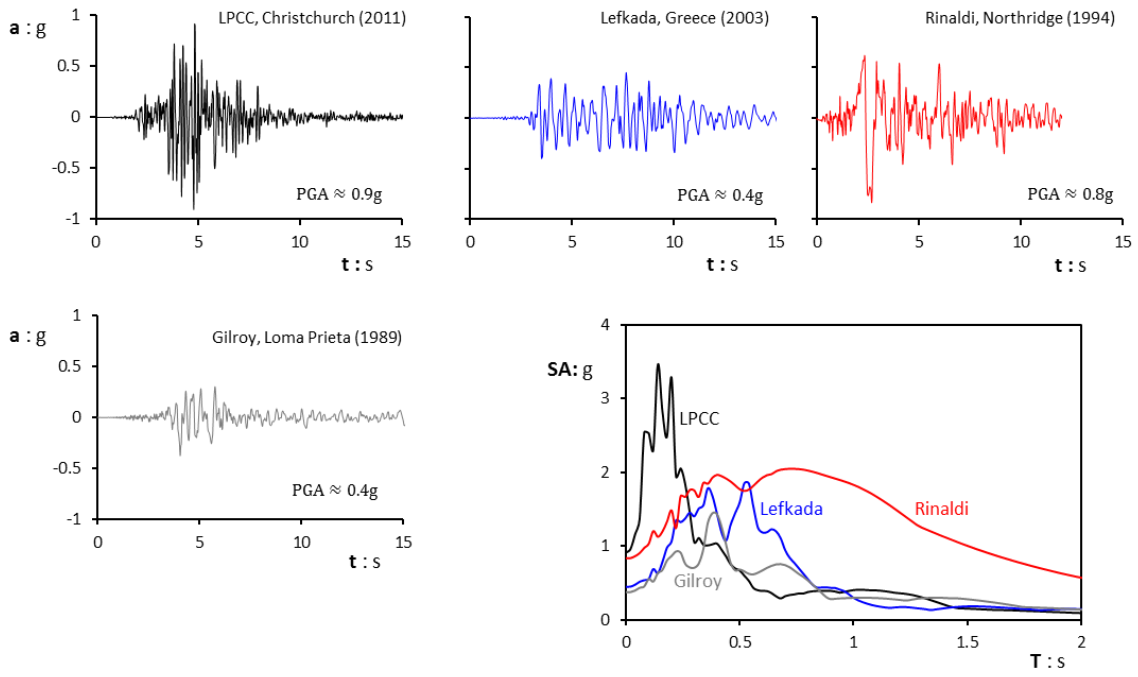

Figure 4. Acceleration time histories used as seismic excitations for the dynamic analysis of the retaining systems and their elastic response spectra.

Figure 5 summarizes the performance of the compared systems in terms of permanent outward horizontal displacements at the end of each earthquake scenario. Taking account of the polarity effect, results are presented for the worst case (left or right wall). It is evident that both walls are less sensitive to the specific high-frequency excitations, while substantial deformations were observed for the low-frequency motions. Nonetheless, in all cases MSE exhibits remarkably lower lateral movements than the concrete pile wall.

A typical result of the Abaqus seismic analysis is portrayed in Fig. 6 in form of contours of plastic strains on the deformed shape of the system. The response of MSE under seismic excitation differs from the static one, governed by an overturning mode of deformation. As such, the maximum lateral movement occurs at the top of the wall, while the reinforced zone moves outwards and rotates imitating the pattern of a rigid block. In addition, the failure surface forms behind the reinforced zone at the backfill and no internal plastic deformation may be observed. On the other hand, the pile deformations seem to follow their pattern under static loading conditions, caused by the formation of an active wedge behind the wall due to the lateral active earth pressures.

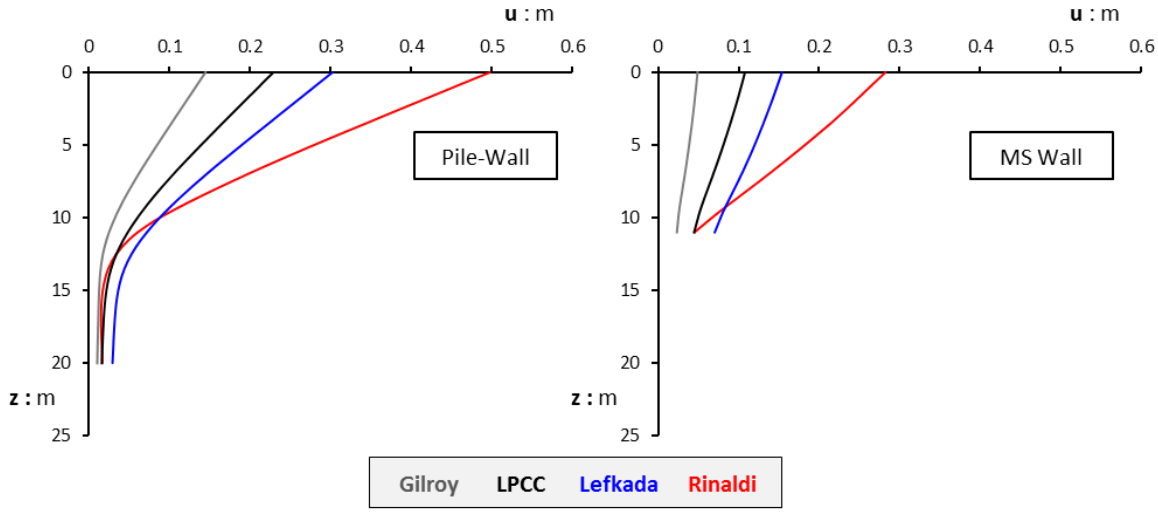

Figure 5. Distribution of the permanent horizontal displacements at the end of the seismic excitations along the wall height.

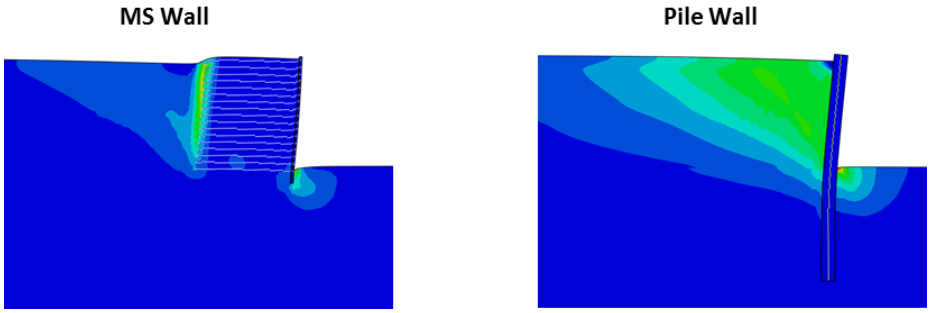

Figure 6. Contours of plastic strains on the deformed mesh at the end of the seismic excitation

Considering the extreme case of the Rinaldi excitation, Fig. 7 compares the acceleration and displacement time histories at the top of each system. It is shown that both retaining systems follow the dynamic deformation of the backfill, allowing the propagation of even high-frequency acceleration pulses to the top, with the more flexible pile alternative experiencing quite larger accelerations. Note that at around t=4.9s (i.e. the instant of the main pulse) the pile wall experiences significantly larger displacement than that of MSE; this displacement remains as irrecoverable residual deformation after the end of shaking, although the displacement attributable to the trailing pulses is practically equal for the two systems. It is obvious that, despite the severity of the event the MSE wall has been able to resist with relatively limited deformations of 27 cm while the piled wall displacement has reached 50cm on its top. Although both systems may seem to have been able to avoid collapse, the deformation of the piled wall would definitely be considered unacceptable by performance standards.

Moreover, the superiority of the MSE system is also luminous in terms of structural distress. Figure 8(a) portrays the moment-curvature plot of the pile produced during shaking, superimposed with its monotonic M-k curve: apparently the pile has developed large curvature values which have led it to expend its available strength, rendering it threateningly vulnerable to a hypothetical next event such as an aftershock. Unfortunately though, an aftershock of quite significant intensity would actually be a high probability scenario after such an extreme event as the Rinaldi shaking. On the other hand, the MSE wall displays an absolutely resilient performance: not only has it been able to sustain the shaking experiencing almost half the displacement of the piled wall, but it has done so while developing stresses well below the steel yield limit of 500MPa at all levels of reinforcement (Fig. 8(b)).

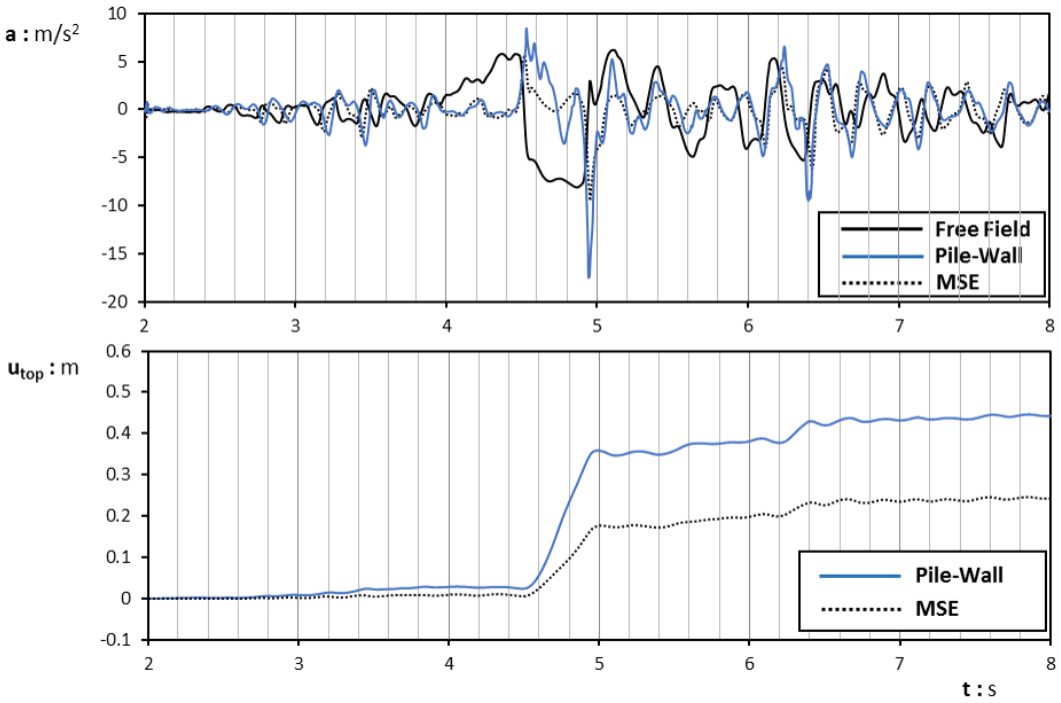

Figure 7. Acceleration and displacement time histories at the top of the retaining structures when subjected to the Rinaldi excitation (Northridge, 1994).

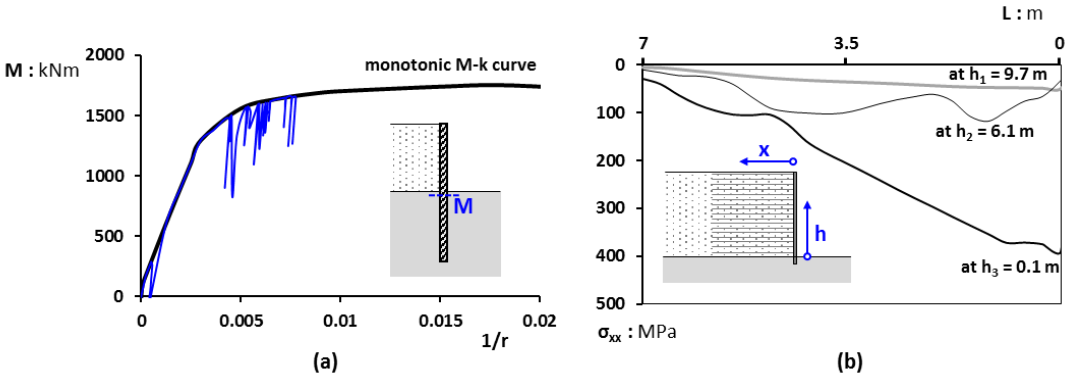

Figure 8. Seismic Performance of the retaining systems when subjected to the extremely strong Rinaldi time-history: (a) Moment-curvature diagram at the point of fixity; (b) axial stresses along the reinforcement length at three characteristic heights (h_1, h_2 and h_3).

MSE wall reliability and redundancy

After highlighting the resilience of MSE retaining walls in terms of their ability to preserve their structural integrity under extremely strong earthquake events and remain functional afterwards, this section briefly investigates the reliability and addresses the redundancy accompanying this system.
To this end, the strength parameters (tanφ and c) both for the retained and the foundation soil were reduced from their initial values, by applying a reduction factor of 1.4, and the retaining systems were then subjected to the Gilroy excitation. Although the maximum increase of their horizontal displacements (Fig 9 (a)) was almost similar, in the case of MSE this increase is almost uniform with height, whereas when examining the pile wall it is concentrated in a single section (or in a small region). This trend results in a non-negligible (of about 40%) increase in the bending moment of the pile, driving the concrete section closest to its ultimate capacity (Fig 9(c)). By contrast, as shown in Fig.9(b) , the axial stresses along the reinforcements do not exceed the steel yield stress, even for the deepest row.

The confidence that the MSE system will perform as intended is further enhanced by the following: the MSE wall is again subjected to the extreme (Rinaldi record) earthquake shaking having preserved only half of the

originally prescribed grids (i.e. grid reinforcements are now considered at vertical distances of 1.2m instead of 0.6m). This setup corresponds to a quite unrealistic scenario where half of the required reinforcements are unable to offer any resistance. Results are plotted in Fig. 10 in terms of distribution of horizontal displacements along the wall, revealing a quite astonishing response. Contrary to the reader's first anticipation, the increase in horizontal displacements is only marginal.

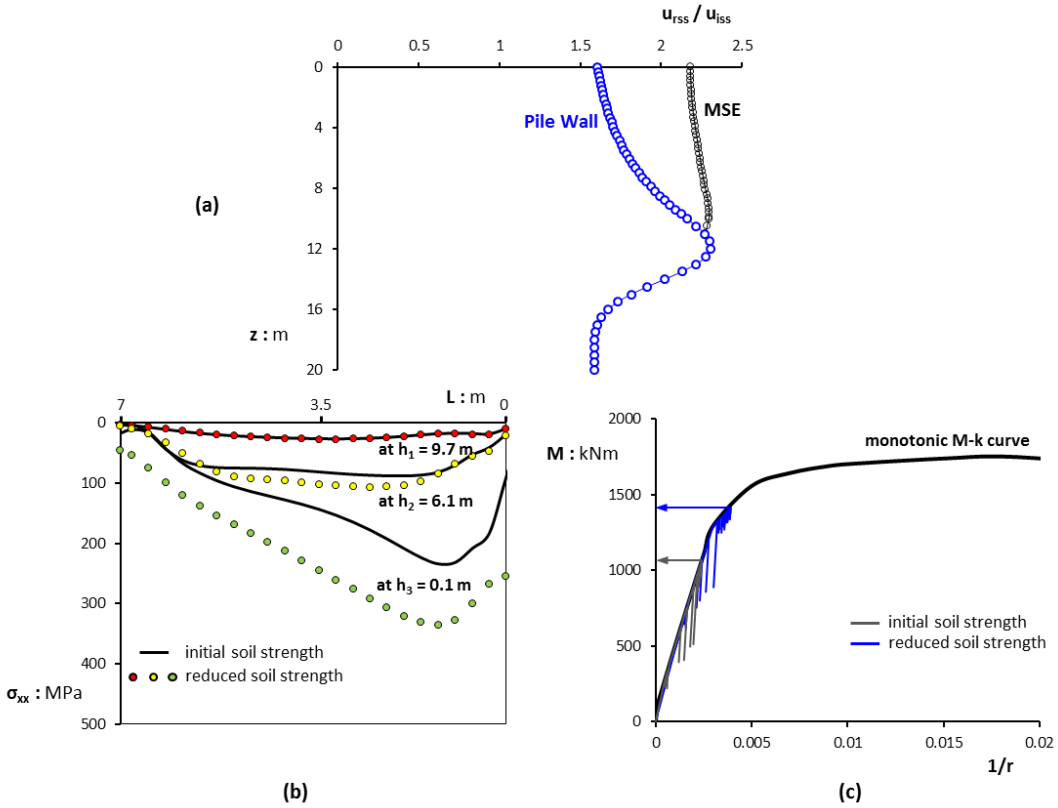

Figure 9. Effect of the soil strength reduction on the response of the compared retaining systems under the Gilroy excitation: (a) ratio of the horizontal displacements for the strength-reduced soil (u_{rss}) over the corresponding for the initial soil (u_{iss}); (b) axial stresses along the reinforcement length at three characteristic heights (h_1, h_2 and h_3); (c) Moment-curvature diagram at the point of fixity.

This excellent response is the result of the transformation of the resisting mechanism: instead of the rigid block response observed in case of the properly designed MSE wall, the system now sustains severe plastic yielding in the "internal" soil (Fig. 10(a)) and obvious distress of the reinforcement bars. Indeed, when properly designed the bars are structurally "underexploited" (i.e. offer their resistance mainly via the friction mechanism) while the internal soil develops no serious strain. These are the two concealed safety fuses which are inherent in this system and provide it with redundancy. Of course, the bottom (more stressed) bar evidently reaches its capacity which is perhaps a sign of imminent failure.

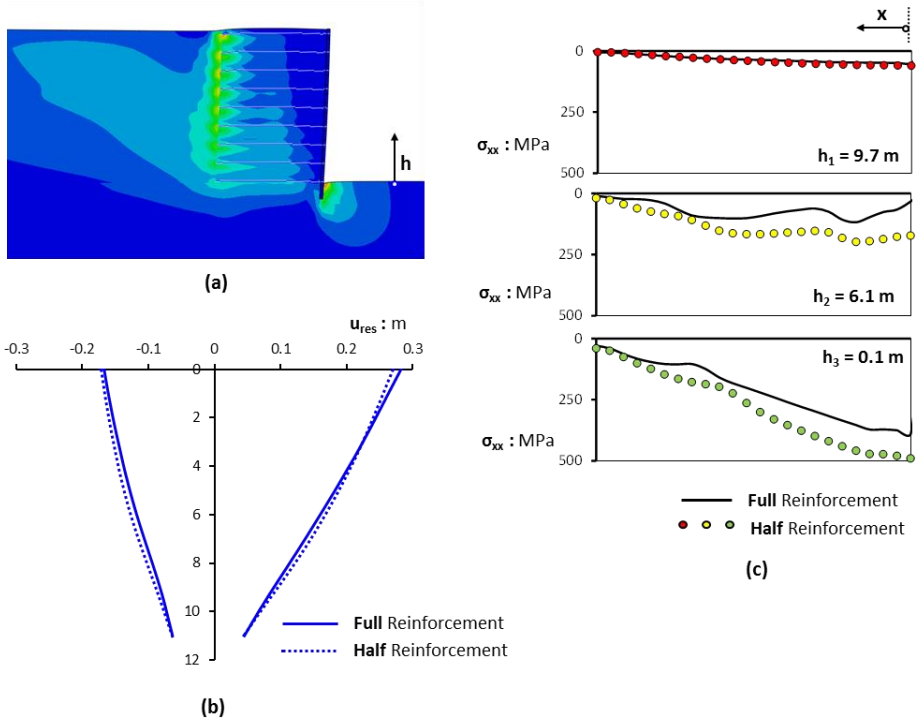

Figure 10. MSE redundancies when the cut is subjected to the Rinaldi excitation: (a) contours of the plastic strain at the end of shaking (assuming that only half of the reinforcement is active); (c) axial stresses along the reinforcement length at three characteristic heights (h_1, h_2 and h_3).

CONCLUSIONS

This paper has comparatively investigated the response of a conventionally designed pile wall and a mechanically stabilized earth wall retaining a vertical soil cut of height H=10m when subjected to several earthquake scenarios. It has been shown that despite the massive dimensions of the piles (diameter D=1.2m and depth L=20m), and despite the fact that both systems have been designed to meet the same state-of-the-art strength-based criteria, the lightweight MSE wall demonstrates a superior performance for all cases examined. The MSE system has been shown to experience remarkably lower displacements while maintaining the structural integrity of the reinforcement bars; on the contrary, the piled wall experiences almost double deformations –especially when subjected to extreme earthquake shaking, while its structural distress renders it extremely vulnerable to any potential aftershock.

Our analyses suggest that the MSE alternative constitutes a resilient retaining structure, owing not only to its superior performance in terms of performance-based indices, such as residual deformations, but also due to its ability to remain operable immediately after an earthquake and its inherent redundancies. The latter come in the form of additional robustness that may be offered by internal soil yielding and exploitation of the total available tensile strength of the reinforcement bars.

REFERENCES

Anastasopoulos, I., Gelagoti, F., Kourkoulis, R., and Gazetas, G., 2012. Simplified Constitutive Model for Simulation of Cyclic Response of Shallow Foundations: Validation against Laboratory Tests. Journal of Geotech. and Geoenv. Engineering, ASCE, 137, No. 12, 1154-1168.

Bolton, 2012. Performance-based design in geotechnical engineering, 52nd Rankine Lecture, London, UK.

Bruneau, M. and Reinhorn, A. M., 2007. Exploring the concept of seismic resilience for acute care facilities, Earthquake Spectra, 28(1): 41-62

Holling, C. S. 1996. Engineering resilience versus ecological resilience. National Academic Press, Washigton DC, USA.

Ishibashi, I., and Zhang, X., 1993. Unified dynamic shear moduli and damping ratios of sand and clay, Soils and Foundations; 33(1), pp. 182-191.

Kramer (2008), “Performance-Based Earthquake Engineering: Opportunities and Implications for Geotechnical Engineering Practice”, Geotechnical Earthquake Engineering and Soil Dynamics IV, Sacramento, California, United States.

Lajevardi, S. H., Dias, D., and Racinais, J., 2013. Analysis of soil-welded steel mesh reinforcement interface interaction by pull-out tests, Journal of Geotextiles and Geomembranes; 40, pp. 48-57.

Seed, H. B., Wong, R. T., Idriss, I. M., and Tokimatsu, K., 1986. Moduli and damping factors for dynamic analyses of cohesionless soils, Journal of Geotechnical Engineering, ASCE, 112(11), pp-1016-32.

Sabermahani, M., Ghalandarzadeh, A., and Fakher, A., 2009. Experimental Study on Seismic Deformation Modes of Reinforced-Soil Walls, Geotextiles and Geomembranes 27 (2), pp. 121-136.